# Low temperature spark plasma sintering of efficient (K,Na)NbO3 ceramics

Christopher Castro Chavarría, Hélène Debéda, Bernard Plano, Lionel Teule-gay, Dominique Michau, Sébastien Fourcade, Mario Maglione, U-Chan Chung, Catherine Elissalde

Journal of the European Ceramic Society xxx (xxxx) xxx

Contents lists available at ScienceDirect

Journal of the European Ceramic Society

journal homepage: www.elsevier.com/locate/jeurceramsoc

# Low temperature spark plasma sintering of efficient (K,Na)$NbO_3$ ceramics

Christopher Castro Chavarría [a,b,*], Hélène Debéda [a], Bernard Plano [a], Lionel Teulé-Gay [b], Dominique Michau [b], Sébastien Fourcade [b], Mario Maglione [b], U-Chan Chung [b], Catherine Elissalde [b]

[a] Univ. Bordeaux, CNRS, Bordeaux INP, IMS, UMR 5218, F-33405 CEDEX Talence, France
[b] Univ. Bordeaux, CNRS, Bordeaux INP, ICMCB, UMR 5026, F-33600 Pessac, France

ARTICLE INFO

*Keywords:*
Potassium Sodium Niobate
KNN
Grain size effect
Dielectric spectroscopy
Spark plasma sintering

ABSTRACT

This study investigates the sintering optimization and characterization of ($K_{0.5}$,$Na_{0.5}$)$NbO_3$ (KNN) ceramics using spark plasma sintering (SPS) at low temperatures. The influence of sintering temperature on crystal structure, microstructure, and dielectric properties is explored. KNN ceramics were sintered as low as 400 °C and exhibit a relative permittivity ($\varepsilon_r$) of 740 and a low dissipation factor (tan(δ)) of 0.02 at room temperature. These findings highlight the potential of SPS-sintered KNN ceramics at low temperatures for applications requiring high permittivity and low dielectric losses.

## 1. Introduction

Lead-free piezoelectric ceramics have garnered significant interest in recent years as environmentally friendly alternatives to traditional lead-based materials. Among the promising lead-free piezoelectric ceramics [1], Potassium Sodium Niobate, ($K_{0.5}$,$Na_{0.5}$)$NbO_3$ (KNN) [2], has gained considerable attention due to its excellent piezoelectric properties. Perovskite KNN ceramics exhibit large piezoelectric activity, making them attractive for applications such as sensors, actuators, and energy harvesting devices [1–4]. However, the sintering of KNN ceramics raises a significant challenge due to the volatility of alkali metals at elevated temperatures [5]. The high vapor pressure of potassium during sintering results in significant loss, leading to a deviation from the stoichiometry and deteriorated electrical properties. Therefore, exploring effective sintering techniques and optimizing the sintering conditions is crucial for obtaining dense and high-performance KNN ceramics [1,3,4].

In recent years, spark plasma sintering (SPS) [6–8], cold sintering process (CSP) [9], hot pressing [10], and microwave sintering [11] have emerged as promising techniques for the processing of advanced ceramics. In the pursuit of sustainable and cost-effective manufacturing, reducing sintering temperatures is crucial to minimize the environmental impact. A drastic reduction in the sintering temperature of KNN below 400 °C would enable the fabrication of piezoelectric devices on flexible substrates such as Kapton®, a versatile polyimide film widely used in electronic applications. The lowest sintering temperature of KNN has been achieved by CSP [9] at the range of 200–400 °C with the addition of hydroxides as fluxes. However, pressure as high as 400 MPa is used and leads to high dislocation densities detrimental to the piezoelectric properties. Moreover, a post-annealing at 700 °C is mandatory to recover optimal direct piezoelectric coefficient values. SPS offers advantages such as rapid heating rates, short processing times, and the ability to control the sintering atmosphere [6,12]. In previous studies, KNN was partially sintered by SPS in the range of 600–800 °C with relative densities from 55% to 86% in order to obtain porous ceramics [13,14]. To obtain highly dense ceramics, KNN has been sintered by SPS as low as 900 °C, but again, a post annealing was necessary in particular to restore the oxygen stoichiometry [13,15–17].

In this study, we focus on the sintering optimization and comprehensive characterization of KNN ceramics working with the SPS technique in a temperature window that has not yet been explored for dense ceramics between 400 and 800 °C [9]. The objective is twofold, to exploit the reactivity of the starting KNN nanoparticles and to avoid post SPS annealing. The influence of the sintering temperature on the crystal structure, microstructure, and electrical properties has been investigated to qualify the obtained ceramics.

## 2. Experimental procedure

Nanometric commercial powder of ($K_{0.5}$,$Na_{0.5}$)$NbO_3$ (KNN) from CerPoTech (Norway) was used as the raw material for its reactivity. To

* Corresponding author at: Univ. Bordeaux, CNRS, Bordeaux INP, IMS, UMR 5218, F-33405 CEDEX Talence, France.
*E-mail address:* christopher.castro-chavarria@u-bordeaux.fr (C.C. Chavarría).

https://doi.org/10.1016/j.jeurceramsoc.2024.01.039
Received 30 June 2023; Received in revised form 19 December 2023; Accepted 12 January 2024
Available online 15 January 2024


Please cite this article as: Christopher Castro Chavarría et al., *Journal of the European Ceramic Society*, https://doi.org/10.1016/j.jeurceramsoc.2024.01.039

sinter samples at 400 °C, the KNN powder was mixed with 10 vol% of NaOH (>98%, Alfa Aesar) and KOH (99.24% trace metals basis, Fisher Scientific) in 1:1 M ratio of K to Na. Ceramic pellets were prepared by SPS using a Syntex Dr. Sinter Lab Model SPS-515S. The 20 nm grain size KNN powder was loaded into a SPS graphite die with a 10 mm inner diameter. The SPS chamber was evacuated to a pressure below 10 Pa prior to heating. The temperature was then raised to the target sintering temperatures (400 °C, 650 °C, 700 °C and 750 °C) at a heating rate of 100 °C/min and maintained under a constant pressure of 100 MPa along the Z-axis on the sample. The dwell time was adjusted in order to obtain high bulk densities (>92%). SPS sintering at 1000 °C was also performed to obtain a reference sample.

The geometric bulk density of the SPS samples was measured and compared to the theoretical value of 4.51 g/cm$^3$.

Crystallinity and phase purity were checked by (XRD) analysis, performed at room temperature on a PANalytical X′pert MPD-PRO Bragg-Brentano θ-θ geometry diffractometer using Cu $K_\alpha$ source.

The microstructure of the fractured ceramics was observed using scanning electron microscopy (SEM, JEOL-ISM-6100, 20 kV). Average grain size was determined by the intersection method.

The dielectric properties were measured using a HP-4194 impedance/gain-phase analyzer in the temperature range of 20 °C to 440 °C. Platinum electrodes were sputtered on both surfaces of disk-shaped pellets (1 ± 0.1 mm thickness and 10 ± 0.1 mm diameter).

## 3. Results and discussion

Fig. 1 shows the XRD patterns of the $(K_{0.5},Na_{0.5})NbO_3$ initial powder and the ceramics prepared by SPS at 400 °C, 650 °C, 700 °C, 750 °C and 1000 °C. The ceramics sintered at the two highest temperatures (i.e. 750 °C and 1000 °C) presented blue coloration directly after SPS and were then annealed at 750 °C and 1000 °C respectively, for 10 h in air. The dwell time was optimized for each sintering temperature in order to systematically reach a relative density above 92% (Table 1).

The diffraction peaks position of the KNN (JAPDS-ICDD file # 00–065-0275) are also shown at the bottom of Fig. 1 with vertical lines for comparison. The diffraction patterns of both initial powder and all the SPS ceramics are identified as orthorhombic crystal structure. Whatever the sintering temperature, no secondary phase was detected by XRD. This suggests that the perovskite phase is preserved after sintering at low temperatures by SPS. Despite the change from the white-colored powder to a dark blue color for the SPSed ceramics above 750 °C, there was no difference in the XRD patterns of both samples, as shown in Fig. 1. The dark blue color is ascribed to oxygen deficiency in its crystal lattices, caused by the low oxygen partial pressure atmosphere of SPS. The annealing treatment in air leads to a change from blue to cream white color, assuming thus the recovery of oxygen stoichiometry. Moreover, the broadening of the peaks {022} and {200} for the SPSed ceramics between 650 °C and 750 °C could be explained by a crystallite size effect resulting from a submicronic microstructure. This broadening does not occur in the ceramic sintered at 400 °C, implying a similar crystallite size to that of the sintered at 1000 °C.

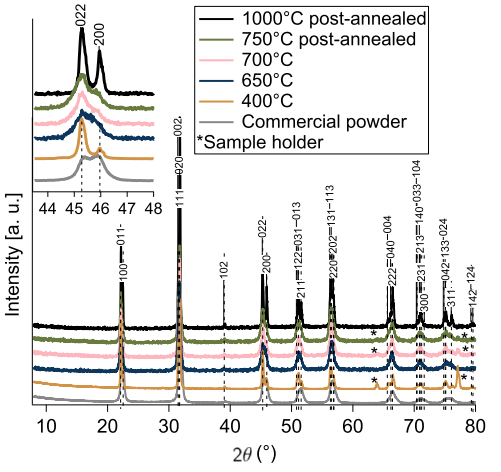


**Fig. 1.** XRD patterns of the initial KNN commercial powder and SPS ceramics sintered at different temperatures. Zoom on the peaks (022) and (200) in the inset.

Fig. 2 shows SEM micrographs of the KNN ceramics SPSed at 400, 650, 700, 750 and 1000 °C. The examination of the fractured surfaces confirms the high density reached whatever the sintering temperature. The average grain size remains submicronic (100–300 nm) for samples sintered between 650 ° and 750 °C, confirming the size effect suggested in XRD section. Grain growth occurs for the samples sintered at 1000 °C which exhibit average grain size in the range of 1–3 μm associated with a change in morphology. Indeed, cubic shaped particles appear as a consequence of growth of the well-rounded grains characteristic of densification at low temperature without sintering aids. It is worth noting that the sample sintered at 400 °C exhibits grain growth and a polydisperse grain size distribution with large cubic grains around 1 μm and submicronic grains. Such microstructure compared to the ones relative to 650 °C and 750 °C is consistent with the {022} and {200} peaks splitting observed. The role of the hydroxides flux towards granular growth is not yet stablished, but an excess of alkalis under specific conditions could promote growth [18]. Additional information on the influence of the flux content is provided in the supplementary information file.

Fig. 3 displays the relative permittivity ($\varepsilon_r$) dependence on the temperature, measured at 100 kHz for the different SPS ceramics. All the curves exhibit two frequency independent maxima corresponding to the orthorhombic-tetragonal phase transition ($T_{O\text{-}T}$ = 482 K) and the tetragonal-cubic phase transition ($T_C$ = 670 K). The phase transition temperatures of the reference ceramics (1000 °C) were found to be lower when compared to KNN single crystals ($T_{O\text{-}T}$ = 488 K, $T_C$ =702 K) [19]. The two transitions become diffuse as much as the sintering temperature is decreased. However, it is noteworthy that the $T_C$ values are in good agreement with those reported in literature for KNN ceramics processed with the SPS (660–680 K) [16,17]. The $T_{O\text{-}T}$ can hardly be precisely identified when the sintering temperature falls below 750 °C. The diffuse character of the transitions is attributed to the small grain size. However, for the 400 °C sample, a steeper orthorhombic to the tetragonal phase transition was observed, probably due to the presence of micron-sized cubic grains.

Focusing on the permittivity values, the SPS KNN ceramics exhibited values lying in the range 600–800 at room temperature (Table 1), and at $T_C$, values are more dependent from the sintering temperature, ranging from 2100 for 650 °C and 7570 for 1000 °C. Note that the value is higher for 400 °C than at 650 °C. For sake of comparison, Wang et al. reported a $T_C$ of 689 K and a room temperature $\varepsilon_r$ of 550 for KNN ceramics prepared by SPS under 60 MPa at 1040–1100 °C for 3 min [20]. These results are quite comparable with the characteristics of our reference ceramics (1000 °C). Even if the permittivity value at room temperature doesn't seem to be affected by the grain size, a drop of the permittivity is observed at $T_C$ from the sintering temperature of 750 °C, and even more pronounced at 650 °C. Here the effect of grain size, residual stress and crystallite size are assumed to be the main cause of these changes since all ceramics are of comparable density. As the grain size decreases, the density of grain boundaries which have lower dielectric permittivity than the core of the grains, is increased. Therefore, the impact of these low permittivity grain boundaries is more visible when the permittivity is greater, i.e. at the $T_C$. In the case of the 400 °C sample, as the crystallite size is similar to that of our reference sample, the polydisperse grain size distribution and the chemistry at the grain boundaries are considered the main cause of the lower permittivity at $T_C$. This softening of the dielectric maxima at the transition temperatures lead to an interesting stabilization of the permittivity over the whole temperature

**Table 1**
SPS conditions of KNN ceramics and their microstructural and dielectric characteristics. Pressure and heating rate are the same for all samples (100 MPa – 100°/min).

| Sint. Temp. [°C] | t [min] | Relative density [%] | Average grain size [nm] | $\varepsilon_r$ at $T_{amb}$ 100 kHz | tan (δ) at $T_{amb}$ 100 kHz | $\varepsilon_r$ at $T_c$ 100 kHz | $T_{O-T}$ [K] | $T_c$ [K] | Color as-SPS | Specific conditions |
|---|---|---|---|---|---|---|---|---|---|---|
| 400 | 10 | 93 | 400 ± 20 | 740 | 0.02 | 2670 | 487 | 677 | Cream | 10% vol. KOH-NaOH |
| 650 | 60 | 92 | 130 ± 10 | 650 | 0.03 | 2100 | - | 667 | White | - |
| 700 | 5 | 96 | 220 ± 20 | 810 | 0.02 | 3150 | - | 666 | White | - |
| 750 | 5 | 97 | 300 ± 20 | 680 | 0.04 | 3180 | - | 670 | Blue | Anneal 750 °C-10 h |
| 1000 | 5 | 98 | 1800 ± 40 | 630 | 0.04 | 7570 | 482 | 669 | Dark blue | Anneal 1000 °C-10 h |

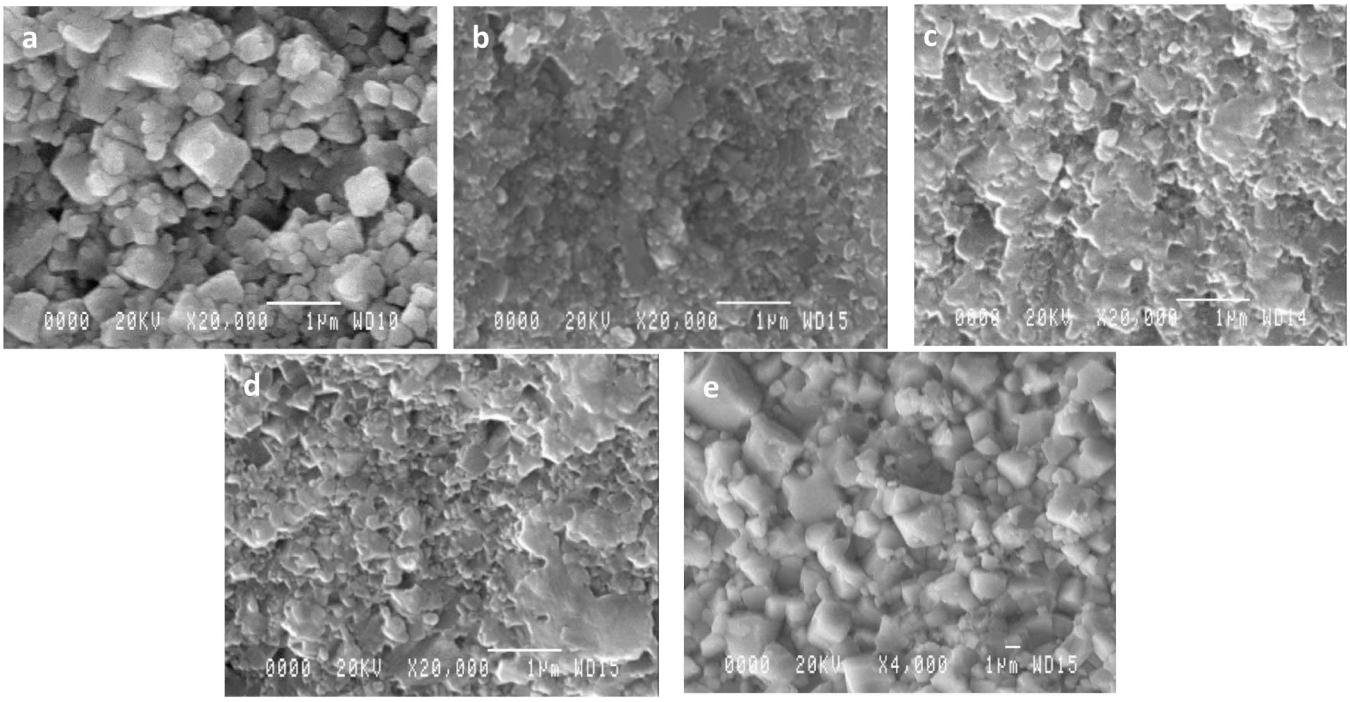


**Fig. 2.** SEM micrographs of the KNN ceramics sintered at (a) 400 °C (b) 650 °C, (c) 700 °C, (d) 750 °C post-annealed and (e) 1000 °C post-annealed (see Table 1 for SPS and annealing conditions).

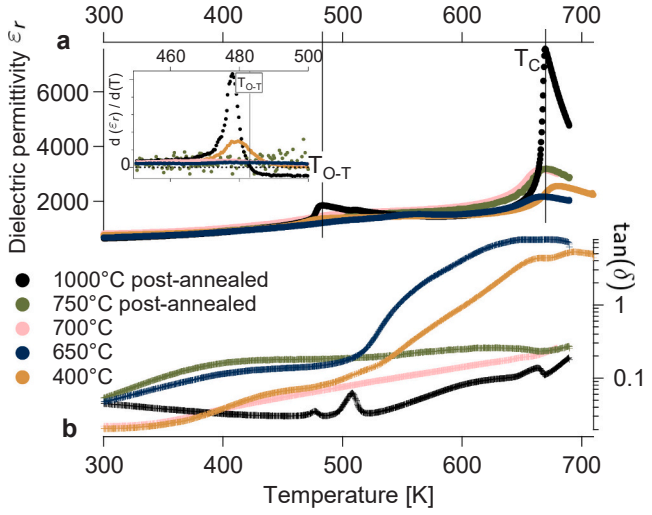


**Fig. 3.** Temperature dependence of (a) dielectric permittivity $\varepsilon_r$ and (b) dielectric losses tan (δ) at 100 kHz for KNN ceramics sintered by SPS. Inset: Permittivity derivative around O-T transition temperature.

range for low sintering temperatures.

The room temperature dissipation factor, for the SPS KNN ceramics was found to be the lowest for the sample sintered at 400 °C and 700 °C (0.02), and higher for the other samples (Table 1). It was reported by Li et al. that the room temperature tan (δ) at 10 kHz of their SPS KNN ceramics was 0.03 [13], whereas Wang et al. observed a value of approximately 0.045 [20].

## 4. Conclusions

In conclusion, we have focused on the sintering optimization and comprehensive characterization of $(K_{0.5},Na_{0.5})NbO_3$ (KNN) ceramics using the SPS technique at low temperatures. Ceramics with comparable density higher than 92% were successfully obtained by targeting SPS temperatures between 650–750 °C without additives and using mild pressure (100 MPa). Only the ceramics obtained at the highest temperatures required a post-annealing. The color change from dark blue to cream white, observed after annealing in air, suggested the supplementation of oxygen deficiency for samples sintered at 750 °C and above. Moreover, we have successfully sintered highly dense KNN ceramics by SPS at an unprecedentedly low temperature of 400 °C, setting a new record for SPS with the utilization of a transient flux, while keeping the pressure as low as 100 MPa. The influence of the sintering temperature on the crystal structure, microstructure, and electrical

properties of the ceramics was investigated and the impact of the grain size was highlighted.

SEM micrographs revealed dense ceramic samples with different grain sizes and shapes according to the sintering conditions. Below 750 °C small rounded grains (<500 nm), are observed, while the sample sintered at 1000 °C exhibits larger cubic grains in the range of 2–3 μm. The sample sintered at 400 °C, presents a large distribution of grain sizes, from submicronic grains to micron-size cubic shaped grains.

The phase transition temperatures of the ceramics were similar to those of KNN sintered by SPS reported in literature, and only slight difference appears according to the sintering temperature.

The relative permittivity ($\varepsilon_r$) values globally increased with the sintering temperature. If the permittivity values are slightly affected by the sintering conditions between room temperature and 500 K, on the other hand a significant drop of the peak of permittivity at $T_C$ is observed.

The specific role of hydroxides flux on both densification and grain growth has to be elucidated. Further, we will investigate the piezoelectric properties of KNN ceramics sintered at low temperatures in order to identify the appropriate compromise in sintering temperature and grain size as it impacts the piezoelectric properties. In depth characterization of the associated grain boundaries will also be addressed.

## CRediT authorship contribution statement

**Christopher Castro Chavarría:** Conceptualization, Data curation, Investigation, Methodology, Software, Visualization, Writing – original draft, Formal analysis, Project administration, Writing – review & editing. **Hélène Debéda:** Conceptualization, Funding acquisition, Validation, Project administration, Resources, Supervision, Writing – review & editing. **Bernard Plano:** Resources. **Lionel Teulé-Gay:** Resources. **Dominique Michau:** Resources. **Sébastien Fourcade:** Resources. **Mario Maglione:** Formal analysis, Writing – review & editing. **U-Chan Chung:** Conceptualization, Formal analysis, Funding acquisition, Validation, Project administration, Resources, Supervision, Writing – review & editing. **Catherine Elissalde:** Conceptualization, Formal analysis, Funding acquisition, Validation, Project administration, Resources, Supervision, Writing – review & editing.

## Declaration of Competing Interest

The authors declare that they have no known competing financial interests or personal relationships that could have appeared to influence the work reported in this paper.

## Acknowledgements

This work was conducted as part of the Post-Petroleum Materials (PPM) project, funded by University of Bordeaux's IdEx "Investments for the Future" program/GPR PPM.

## Appendix A. Supporting information

Supplementary data associated with this article can be found in the online version at doi:10.1016/j.jeurceramsoc.2024.01.039.

## References

[1] J. Rödel, K.G. Webber, R. Dittmer, W. Jo, M. Kimura, D. Damjanovic, Transferring lead-free piezoelectric ceramics into application, J. Eur. Ceram. Soc. 35 (6) (2015) 1659–1681.
[2] Y. Saito, H. Takao, T. Tani, T. Nonoyama, K. Takatori, T. Homma, T. Nagaya, M. Nakamura, Lead-free piezoceramics, Nature 432 (2004) 84–87.
[3] J. Wu, D. Xiao, J. Zhu, Potassium-sodium niobate lead-free piezoelectric materials: past, present, and future of phase boundaries, Chem. Rev. 115 (7) (2015) 2559–2595.
[4] C.-H. Hong, H.-P. Kim, B.-Y. Choi, H.-S. Han, J.S. Son, C.W. Ahn, W. Jo, Lead-free piezoceramics – Where to move on? J. Mater. 2 (1) (2016) 1–24.
[5] H. Birol, D. Damjanovic, N. Setter, Preparation and characterization of (K0.5Na0.5) NbO3 ceramics, J. Eur. Ceram. Soc. 26 (6) (2006) 861–866.
[6] T. Hungria, J. Galy, A. Castro, Spark plasma sintering as a useful technique to the nanostructuration of piezo-ferroelectric materials, Adv. Eng. Mater. 11 (8) (2009) 615–631.
[7] J.A. Eiras, R.B.Z. Gerbasi, J.M. Rosso, D.M. Silva, L.F. Cotica, I.A. Santos, C. A. Souza, M.H. Lente, Compositional design of dielectric, ferroelectric and piezoelectric properties of (K,Na)NbO3 and (Ba, Na)(Ti,Nb)O3 based ceramics prepared by different sintering routes, Materials 9 (3) (2016) 1–12.
[8] J.G. Noudem, D. Kenfaui, D. Chateigner, M. Gomina, Toward the enhancement of thermoelectric properties of lamellar Ca3Co4O9 by edge-free spark plasma texturing, Scr. Mater. 66 (5) (2012) 258–260.
[9] K. Tsuji, Z. Fan, S.H. Bang, S. Dursun, S. Trolier-McKinstry, C.A. Randall, Cold sintering of the ceramic potassium sodium niobate, (K0.5Na0.5)NbO3 and influences on piezoelectric properties, J. Eur. Ceram. Soc. vol. 42 (2022) 105–111.
[10] R.E. Jaeger, L. Egerton, Hot pressing of potassium-sodium niobates, J. Am. Ceram. Soc. vol. 45 (n 5) (1962) 209–213.
[11] M. Feizpour, H.B. Bafrooei, R. Hayati, T. Ebadzadeh, Microwave-assisted synthesis and sintering of potassium sodium niobate lead-free piezoelectric ceramics, Ceram. Int. vol. 40 (nº 1) (2014) 871–877.
[12] Z.A. Munir, U. Anselmi-Tamburini, M. Ohyanagi, The effect of electric field and pressure on the synthesis and consolidation of materials: a review of the spark plasma sintering method, J. Mater. Sci. 41 (3) (2006) 763–777.
[13] J.-F. Li, K. Wang, B.-P. Zhang, L.-M. Zhang, Ferroelectric and Piezoelectric Properties of Fine-Grained Na0.5K0.5NbO3 Lead-Free Piezoelectric Ceramics Prepared by Spark Plasma Sintering, J. Am. Ceram. Soc. vol. 89 (nº 2) (2006) 706–709.
[14] K. Zlouzeova, S. Hribalova, V. Necina, W. Pabst, M. Mika, J. Petrasek, Partially sintered lead-free ceramics from piezoelectric powders prepared via conventional firing and spark plasma sintering (SPS) characterization of microstructure and dielectric properties, Ceram. -Silikáty vol. 65 (n 1) (2021) 30–37.
[15] M. Bah, F. Giovannelli, F. Schoenstein, G. Feuillard, E. Le Clezio, I. Monot-Laffez, Synthesis, microstructure and electromechanical properties of undoped (K0.5Na0.5)NbO3, Adv. Appl. Ceram. 114 (4) (2015) 211–219.
[16] M.M. Gomes, R. Vilarinho, R. Pinho, A. Almeida, J.G. Noudem, M.E.V. Costa, P. M. Vilarinho, J.A. Moreira, Revisiting the phase sequence and properties of K0.5Na0.5NbO3 ceramics sintered by different processes, Ceram. Int. vol. 47 (2021) 8308–8314.
[17] R. Pinho, A. Tkach, S. Zlotnik, M.E. Costa, J. Noudem, I.M. Reaney, P.M. Vilarinho, Spark plasma texturing: A strategy to enhance the electro-mechanical properties of lead-free potassium sodium niobate ceramics, Applied, Mater. Today vol. 19 (2020) 100566.
[18] P. Pop-Ghe, N. Wolff, A. Rubab, L. Kienle, E. Quandt, Tailoring growth modes by excess alkali addition in magnetron sputtered, Materials Today, Communications vol. 27 (2021) 102221.
[19] M.A. Rafiq, M.E. Costa, P.M. Vilarinho, Establishing the domain structure of (K0.5Na0.5)NbO3 (KNN) single crystals by piezoforce-response microscopy, Sci. Adv. Mater. vol. 6 (n 3) (2014) 426–433.
[20] R. Wang, R. Xie, T. Sekiya, Y. Shimojo, Fabrication and characterization of potassium–sodium niobate piezoelectric ceramics by spark-plasma-sintering method, Mat. Res. Bull. vol. 39 (n 11) (2004) 1709–1715.